

N-Guanidyl and C-Tetrazole Leu-Enkephalin Derivatives: Efficient Mu and Delta Opioid Receptor Agonists with Improved Pharmacological Properties

Jean-Louis Beaudeau,[†] Véronique Blais,[‡] Brian J. Holleran,[‡] Alexandre Bergeron,[‡] Graciela Piñeyro,^{||} Brigitte Guérin,^{*,§} Louis Gendron,^{*,‡} and Yves L. Dory^{*,†}

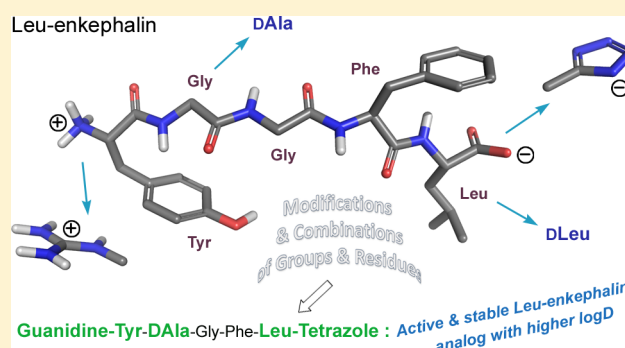
[†]Département de chimie, [‡]Département de Pharmacologie-Physiologie, and [§]Département de Médecine Nucléaire et Radiobiologie, Institut de Pharmacologie, Centre de recherche du CHUS, Université de Sherbrooke, 3001, 12e Avenue Nord, Sherbrooke, Québec J1H 5N4, Canada

^{||}Département de Psychiatrie, Centre de Recherche du CHU Ste-Justine, Université de Montréal, Montréal, Québec H3T 1J4, Canada

S Supporting Information

ABSTRACT: Leu-enkephalin and D-Ala₂-Leu-enkephalin were modified at their N- and C-termini with guanidyl and tetrazole groups. The resulting molecules were prepared in solution or by solid phase peptide synthesis. The affinity of the different analogues at mu (MOP) and delta opioid receptors (DOP) was then assessed by competitive binding in stably transfected DOP and MOP HEK293 cells. Inhibition of cAMP production and recruitment of β -arrestin were also investigated. Finally, lipophilicity (logD_{7.4}) and plasma stability of each compound were measured. Compared to the native ligands, we found that the replacement of the terminal carboxylate by a tetrazole slightly decreased both the affinity at mu and delta opioid receptors as well as the half-life. By contrast, replacing the ammonium at the N-terminus with a guanidyl significantly improved the affinity, the potency, as well as the lipophilicity and the stability of the resulting peptides. Replacing the glycine residue with a D-alanine in position 2 consistently improved the potency as well as the stability of the analogues. The best peptidomimetic of the whole series, guanidyl-Tyr-D-Ala-Gly-Phe-Leu-tetrazole, displayed sub-nanomolar affinity and an increased lipophilicity. Moreover, it proved to be stable in plasma for up to 24 h, suggesting that the modifications are protecting the compound against protease degradation.

KEYWORDS: Delta opioid receptor, pain, peptides, tetrazole, guanidine, lipophilicity, isostere, pharmacological properties, plasma stability.



INTRODUCTION

Chronic pain is one of the most frequent causes of medical advice seeking. Each year the direct cost of chronic pain amounts to about \$560 billion in the United States alone.¹ The neuronal networks involved in pain processing are well-known, and their investigation has led to the identification of numerous potential targets to alleviate pain.^{2–7} However, despite the huge number of molecules developed, mu opioid agonists such as morphine remain the gold standard. Opioid receptors exist at least in three subtypes named mu (MOP), delta (DOP), and kappa (KOP).^{8,9} Several studies suggest that selective activation of DOP could provide good analgesia without the adverse effects linked to traditional MOP-activating opioids.^{10–13} Based on these studies, the hypothesis that the selective activation of DOP would lead to a better therapeutic profile is generally acknowledged.^{14–16} Therefore, great efforts have been made during the last decades. However, many DOP-selective agonists were shown to produce non-

lethal convulsions in rodents and nonhuman primates.¹⁷ Interestingly, recent advance revealed that not all DOP agonists induce convulsions.^{13,18,19} Indeed, some nonpeptide candidates even reached clinical trials for the treatment of pain or depression. However, these were ultimately discarded, because of a lack of efficiency in humans.¹⁹

Owing to their high affinity for DOP, their lack of MOP-related adverse effects, their structural simplicity, and their low toxicity, many efforts were also directed toward endogenous peptides such as enkephalins (Tyr-Gly-Gly-Phe-Leu/Met), deltorphins (Tyr-D-Ala-Phe-Asp/Glu-Val-Val-Gly-NH₂), and their optimization as druggable molecules. Unfortunately, their peptide bonds are easily metabolized by peptidases (half-life of ~2 min)²⁰ and prevent them from crossing the

Received: October 14, 2018

Accepted: January 7, 2019

Published: January 7, 2019

blood-brain barrier (BBB) to reach the central nervous system (CNS), where the key opioid receptors related to analgesia are located.⁸

Over the last decades, different strategies aiming to improve the pharmacokinetic profile of enkephalins were used with limited success. Among them, macrocyclization²¹ has led to selective DOP peptides such as H-Tyr-c[D-Pen-Gly-Phe-D-Pen]-OH (DPDPE)²² and H-Tyr-c[D-Cys-Phe-D-Pen]-OH (JOM-13)²³ with improved stability but still suffering from poor BBB penetration. A useful strategy to increase peptide stability is to replace dipeptides with isosteres. We have already successfully carried such studies on the backbone of Leu-enkephalin (LENK) by replacing each amide bond by different dipeptide isosteres (ester, *N*-methyl amide, triazole, alkene, and fluoroalkene).^{24–28} Together, these studies have been of a great help to uncover the interactions necessary for LENK to fold into its bioactive conformation in the DOP.

Surprisingly, few studies have been conducted on the isosteric replacement of both ammonium and carboxylate N- and C-termini of enkephalins.²⁹ These positions are particularly interesting since enzymatic degradation of enkephalins occurs mostly at these sites.^{20,30} Furthermore, the carboxylate and the ammonium are the main functions responsible for the low bioavailability of enkephalins. Because of their important roles for both the biological activity and selectivity,^{31–33} candidates were chosen cautiously, according to their ability to mimic the ionic state of the endogenous ligand at physiological pH (Figure 1). Thus, tetrazole is a well-suited analogue of a

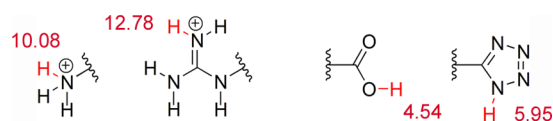


Figure 1. pK_a values of ammonium cation, carboxylic acid, and their respective isosteres guanidine and tetrazole.

carboxylic acid. Indeed, their properties such as size, acidity, and ability to form a H-bond are similar. Consequently, tetrazole could easily replace the free carboxylate group at the C-terminal position, improving at the same time lipophilicity and stability while keeping the key molecular interactions within the receptor. This carboxylate/tetrazole relationship has already been investigated by Manturewicz et al.,²⁹ but surprisingly the study was limited to pharmacodynamics. Recently, Weltrowska et al.³⁴ described the synthesis of mixed mu agonist/delta antagonist compounds, where the free ammonium group was replaced by a guanidinium cation. Such replacement led to a higher cationic profile (increased pK_a) and a higher membrane permeability via association with BBB capillaries.^{35,36} In addition, biological switching from DOP antagonism to agonism was observed. The same strategy was applied to cyclic deltorphins,³⁷ with similar observations concerning their biological activity and pharmacokinetics. To date, such strategies have not been explored for enkephalin derivatives. Such modifications could however improve both the BBB permeability and the stability of the analogues.³⁸ Homologation of the Gly-2 residue with a D-amino acid is also known to be a valid strategy to improve pharmacokinetic and selectivity in compound such as H-Tyr-D-Ala-Gly-Phe-D-Leu-OH (DADLE),³⁹ H-Tyr-D-Ser-Gly-Phe-Thr-OH (DSLET),⁴⁰ and H-Tyr-D-Thr-Gly-Phe-Thr-OH (DTLET).⁴¹ The latter

approach has been combined here to N- and C-terminal modifications of LENK.

In this report, we present the synthesis, affinity, and activity of several enkephalin analogues containing one, two, or three modifications on their structure, and the influence of these combinations on their affinity and potency at MOP and DOP as well as on their lipophilicity and plasmatic stability.

RESULTS AND DISCUSSION

Leu-enkephalin (LENK) is one of the endogenous opioid peptides, often considered as the natural ligand for DOP.⁴² However, as most peptides it has a low bioavailability when systemically administered and is readily degraded by enkephalinases and other peptidases.^{20,43–45} These limitations have to be addressed to transform such peptides into druggable molecules. In line with our previous studies, we systematically replaced each amide bond by dipeptide isosteres, resulting in peptidomimetics with improved stability profiles.^{24–27} Another important aspect not previously considered is the neutral/ionic state of both LENK ammonium and carboxylate termini. Indeed, at physiological pH, LENK is a zwitterion with high hydrophilicity. Furthermore, the first positions to be degraded are the first, the second and the fourth amide bonds.⁴⁶ Replacing the N- and C-termini of LENK by unnatural bioisosteric functional groups should increase its resistance toward degrading enzymes. Tetrazole and guanidyl groups were selected to respectively replace carboxylate and ammonium ions.

Chemistry. The two monosubstituted peptidomimetics **2**, **3** and the disubstituted analogue **4** were synthesized, and their affinities and other relevant properties could be compared to LENK **1** (Figure 2). The tetrazole derivative **2** was found to bind DOP and MOP with a lower affinity than compounds **1**, **3**, and **4**; therefore, additional modifications involving residues Gly2 and Leu5 were later applied to **2**. These two positions are known to impact positively the affinity of LENK derivatives as in DADLE, bearing D-Ala and D-Leu residues at positions 2 and 5, respectively.³⁹ Thus, two new tetrazole derivatives, **5** and **6**, with D-Ala2 and D-Leu5, respectively, were prepared. Subsequently, the tetrazole mimetic **7** combining D-Ala2 and D-Leu5 in the same structure was also prepared. When compared to the D-Leu5 substituted compound **6**, the D-Ala2 analogue **5** led to the best binding results. Finally, the three optimal modifications (from **3** and **5**) were incorporated in the last structure of this series to give rise to compound **8**, a guanidylated LENK containing a tetrazole mimetic at its N-terminus and a D-Ala at position 2.

Synthesis. The tetrazole modified Fmoc-leucines **12a** and **12b** were synthesized in a straightforward fashion as described by Sureshbabu et al.⁴⁷ (Scheme 1). First, the carboxylic acids **9a** and **9b** were efficiently converted to their amides **10a** and **10b**, before being converted to their corresponding nitriles **11a** and **11b**. The latter were transformed into the tetrazoles **12a** and **12b** (click chemistry) with overall yields of 69% and 56% from **9a** and **9b**, respectively.

These modified Fmoc-leucines **12a** and **12b** were coupled overnight on 2-chlorotrityl resin through their tetrazole group,⁴⁸ with an overall loading of 80%. Solid phase synthesis then processed in an iterative way until completion of the peptide sequences (Scheme 2), using an Fmoc strategy. For peptides **1**, **2**, and **5–7**, Boc-Tyr-OH was introduced in the N-terminal position instead of Fmoc-Tyr-OH to remove

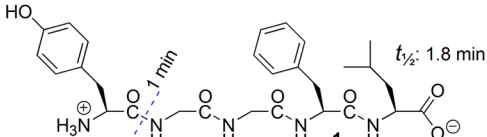
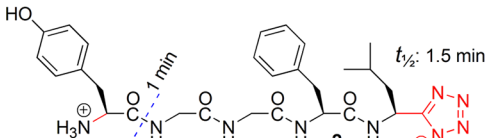
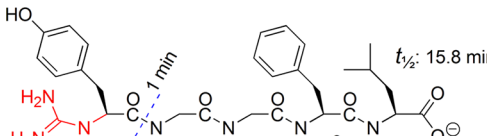
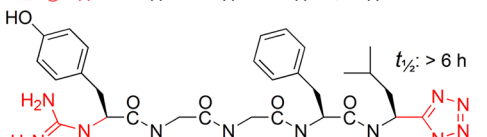
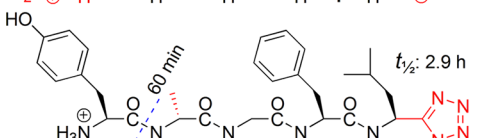
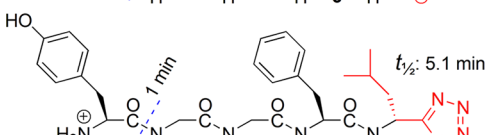
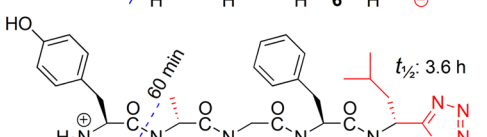
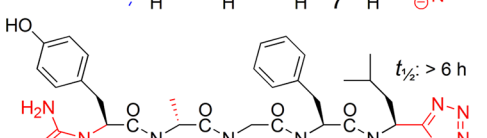
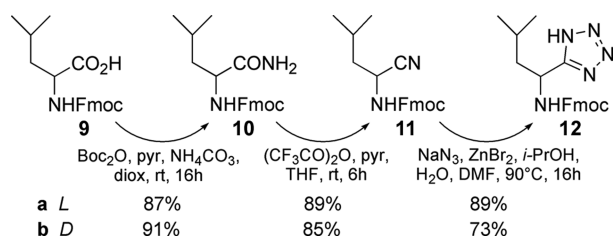
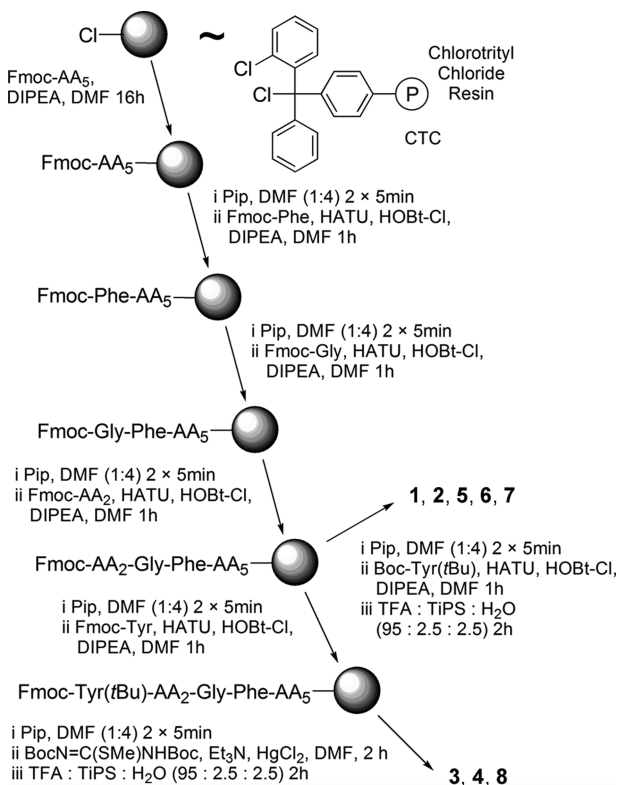
		<i>in vitro</i> affinities		<i>in vitro</i> potencies			
		K_i (nM)		EPAC		β -arrestin	
				EC ₅₀ (nM)	E _{max} (% LENK)	EC ₅₀ (nM)	E _{max} (% LENK)
	DOP	0.41 ± 0.08	0.15 ± 0.03	99.9 ± 0.1	2.66 ± 1.62	99.9 ± 0.2	
	MOP	0.32 ± 0.07	0.89 ± 0.45	100.0 ± 0.2	485 ± 82	100.0 ± 0.3	
	DOP	1.24 ± 0.51	2.87 ± 0.84	113.4 ± 8.8	27.5 ± 9.06	99.6 ± 3.9	
	MOP	2.22 ± 0.55	15.7 ± 6.09	104.7 ± 0.9	2904 ± 1562	87.6 ± 6.7	
	DOP	0.29 ± 0.15	0.18 ± 0.10	99.9 ± 7.9	5.32 ± 1.96	102.5 ± 5.3	
	MOP	0.05 ± 0.02	0.74 ± 0.33	95.7 ± 8.2	304 ± 454	108.3 ± 7.4	
	DOP	1.61 ± 0.44	0.85 ± 0.24	100.9 ± 3.5	71.6 ± 18.9	102.7 ± 3.9	
	MOP	0.25 ± 0.10	2.33 ± 1.04	90.1 ± 6.4	1440 ± 603	104.4 ± 5.5	
	DOP	0.36 ± 0.13	0.25 ± 0.12	104.7 ± 7.5	3.02 ± 0.46	105.5 ± 6.7	
	MOP	0.24 ± 0.07	0.60 ± 0.38	114.3 ± 7.6	685 ± 117	107.6 ± 7.3	
	DOP	3.10 ± 0.76	3.32 ± 2.30	111.4 ± 1.8	92.4 ± 19.2	97.1 ± 4.7	
	MOP	3.03 ± 0.52	10.4 ± 4.8	101.8 ± 4.6	1848 ± 546	97.1 ± 5.8	
	DOP	1.41 ± 0.50	0.49 ± 0.04	106.7 ± 10.2	17.9 ± 7.2	98.7 ± 6.4	
	MOP	0.29 ± 0.06	1.07 ± 0.34	100.2 ± 2.9	356 ± 178	108.7 ± 4.9	
	DOP	0.32 ± 0.07	0.10 ± 0.06	95.2 ± 3.7	13.2 ± 2.7	99.3 ± 2.5	
	MOP	0.20 ± 0.06	0.38 ± 0.29	98.2 ± 7.8	278 ± 83	111.2 ± 8.5	

Figure 2. Structures, *in vitro* affinities, *in vitro* potencies, and rat plasma stability of target peptides 1–8. The binding affinity (K_i) of each compound was determined by their ability to inhibit the binding of [¹²⁵I]-deltorphin I and [¹²⁵I]-DAMGO, used as selective radioligands, respectively, for DOP and MOP (K_d = 0.13 nM Delt I and K_d = 0.69 nM DAMGO). Membrane preparations of stably transfected HEK cells were used. K_i values are the means ± SEM of three to six independent experiments, each performed in duplicate. Potency (EC₅₀) and the efficacy (E_{max}) of each compound were determined by their respective ability to inhibit the forskolin-induced cAMP production through both DOP and MOP, using the GFP10-EPAC-RLucII BRET biosensor. Potency of each compound to recruit β -arrestin 2 using the GFP10-arrestin DOP/MOP-RLucII BRET couple. EC₅₀ values are the means ± SEM of three to five independent experiments each performed in triplicate. Half-life time ($t_{1/2}$) or rat plasma stability of each compound was measured at 37 °C (ex-vivo) on an analytical Water H Class Acquity UPLC coupled with a SQ detector 2 and a PDA eλ detector (200 to 400 nm) and paired with an Acquity UPLC CSH C18 column, 1.7 μ M, 2.1 Å ~ 50 mm, flow 0.8 mL/min, starting with 0.1% formic acid in water, then moving to 95% acetonitrile containing 0.1% formic acid in 1.3 min. Degradation fragments were identified through MS analysis, and their first appearance time is shown at the cleavage site.

simultaneous the N-terminal protective group during the resin cleavage.

For the replacement of the ammonium by a guanidinium (as in peptides 3, 4, and 8), the most popular procedures usually require cleavage of peptides from the resin, followed by an orthogonal protection in the C-terminal position and the conversion of the amine to the guanidine in one or several

steps.³⁷ These multiple steps make the synthesis workflow somehow cumbersome. On the other hand, solid-phase protocols described in the literature are often expensive⁴⁹ or suffer from poor efficiency^{50,51} and/or side reactions^{52,53} in addition to being dependent on solvents or steric hindrance.^{54,55} Nevertheless, we opted for the solid phase approach due to its reduced number of steps. We succeeded

Scheme 1. Synthesis of Modified Fmoc-Leucine-Tetrazoles 12a and 12b**Scheme 2. Solid Phase Peptide Synthesis Protocol**

in applying such methodology using Mukaiyama's conditions with *N,N*-diBoc-methyl-thio-isourea as guanidylating agent and HgCl₂ as reducing agent (Scheme 2).^{52,53}

Total conversion was observed after 2 h (occasionally, the procedure needed to be repeated twice for completion). The cytotoxicity of mercury chloride was not an issue, since it could easily be removed by filtration due to its high solubility in DMF. As a result, these optimized conditions for solid phase synthesis allowed us to rapidly obtain all the compounds of our library in a convergent way.

Binding Properties and Activity on DOP and MOP. To evaluate the ability of each compound to bind DOP and MOP, we performed competitive binding assays using membrane preparations from transfected HEK cells expressing either DOP (HEK/DOP) or MOP (HEK/MOP). Leu-enkephalin 1 and compounds 2–8 inhibited the binding of [¹²⁵I]-deltorphan 1 (on DOP) and [¹²⁵I]-DAMGO (on MOP) in a concentration-dependent manner (Figure 2). The replacement of the carboxylate by a tetrazole in compounds 1 and 3, to produce the derivatives 2 and 4, respectively, led to a slight decrease in affinity. When a guanidinium was introduced in LENK instead of the ammonium to get compound 3, affinity was improved

with a significant preference for MOP. This selectivity trend was confirmed when a guanidyl group was included in addition to tetrazole in compound 4.

After the preliminary exploration involving the two ends of LENK, additional modifications were introduced at its second and fifth residues. Thus, starting from peptide 2, Gly2 was replaced by a D-Ala2 residue in mimetic 5 and the chirality of modified (tetrazole) Leu5 was inverted in 6. The two changes were then combined in the analogue 7. From the K_i values measured for the four compounds 2, 5–7, we could easily conclude that D-Ala at position 2 is indeed a favorable element for binding to DOP, whereas inversion of the side chain of the fifth residue is not.

Finally, features perceived as beneficial were combined in analogue 8, which can be seen as 4 with added D-Ala2 or 5 with ammonium-guanidinium replacement. Compound 8 was found to be very potent, being as good as 3 and 5, and slightly better than LENK 1. Overall, the four molecules 1 (the reference ligand), 3, 5 and 8 have a good affinity for both DOP and MOP.

Following the determination of the binding affinity of the library, the potency of each compound was assessed. Activation of the opioid receptors by their ligands initiates a cascade of intracellular reactions.⁵⁶ One of these phenomena is the inhibition of adenylate cyclase through the activation of the G_i protein,⁵⁷ resulting in a decrease in the cAMP production. To monitor changes in second messenger levels, we used a BRET-based biosensor in which acceptor (GFP10) and donor (RLucII) moieties were, respectively, introduced at the N- and C-terminal ends of the protein EPAC (GFP10-EPAC-RLucII), used here as a cAMP sensor.⁵⁸ cAMP produced in the presence of forskolin (3 μM) imposes conformational changes to the biosensor which, in turn causes a reduction of the BRET signal. Once activated,⁵⁹ opioid receptors are also phosphorylated, leading to the recruitment of β-arrestin.⁶⁰ The β-arrestin pathway is involved, among other processes, in receptor internalization and downregulation and is thought to be responsible for the deleterious effects of opioids^{61–63} (although this has been challenged by recent findings TRV130 and PZM21).^{64,65} A second signaling outcome that was studied was therefore the recruitment of β-arrestin 2-GFP10 to DOP or MOP bearing RLucII in their C-terminus. All tested compounds showed full agonist activity for the EPAC and β-arrestin pathway (Figure 2; Emax). Potencies followed the same trend as binding affinities (Figure 2). Almost all compounds are less potent than LENK, except for compound 8, indicating that, once again, the best results were obtained with the latter derivative.

As shown in Figure 2, when compared to LENK 1, for most compounds a higher concentration was required to recruit β-arrestin. Interestingly, compounds 3 and 5, and to a lesser extent 7 and 8, behave much like LENK itself (compound 1). When all the characteristics (guanidyl, tetrazole, D-Ala2) of these three analogues are included in one structure (compound 8), the β-arrestin pathway becomes slightly disfavored, at least with DOP. Generally speaking, the chosen modifications (apart from D-Leu5) thus prevent any major change in affinity and potency when compared to LENK.

Molecular Modeling. To better understand our binding results, compounds 1–8 were docked into the Human Delta Opioid Receptor crystallographic structure 4N6H,³¹ following the Induced Fit Docking (IFD) algorithm. The ligands were given full mobility, whereas the receptor itself was allowed to

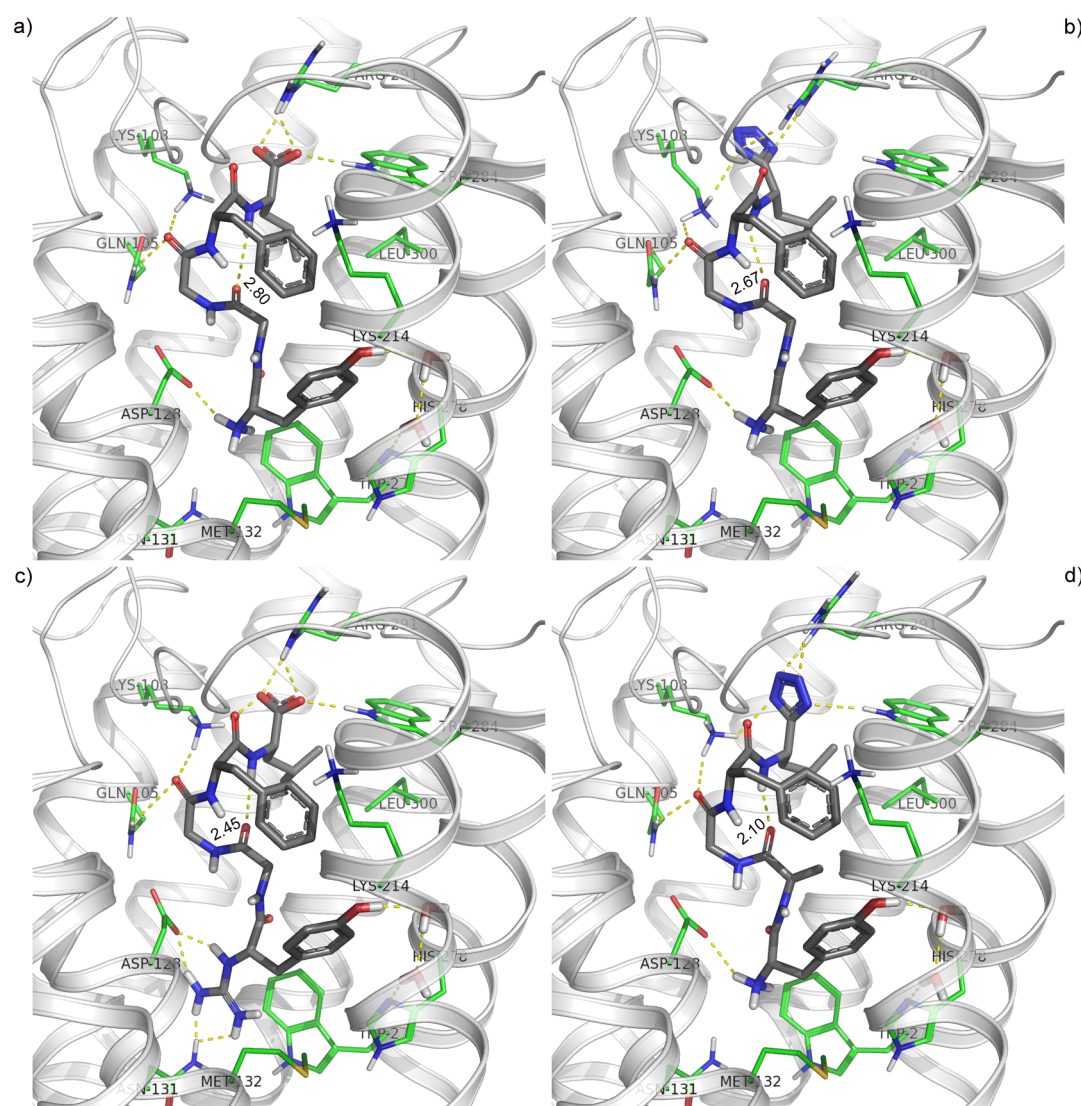


Figure 3. Induced Fit Docking snapshots of compounds 1–3 and 5 in DOP. Side chains were allowed full mobility. Distances for the β -turn (between second and fifth residues) of the ligands are indicated (Å). (a) LENK 1. (b) Compound 2. (c) Compound 3. (d) Compound 5.

freely adjust the geometry of its side chains to a distance of 15 Å away from the docked ligands. Three regions are of particular importance, the N- and C-terminal positions of the ligands, as well as the second residue. (Figure 3).

These three locations were thoroughly scrutinized since the following modifications from LENK 1: amine \rightarrow guanidine (at the N-terminus), Gly \rightarrow D-Ala (at position 2) and carboxylic acid \rightarrow tetrazole (at the C-terminus) led to the best compound (compound 8) of the whole series. With respect to the C-terminus, we found that the interactions between the carboxylate of 1 (Leu5) and the receptor are essentially retained in its tetrazole mimetic (compound 2) (compare Figure 3a and b). More specifically, both groups similarly interact with the side chain of Arg290 through a salt bridge. The negatively charged groups of compounds 1 and 2 are further held in place by additional interactions with Trp284 and Lys108, respectively. As for the N-termini, the essential salt bridge between the ammonium (Tyr1) and Asp128 and the two water molecules linking the phenol group (Tyr1) and His278 are conserved with the guanidyl replacement (compare Figure 3a and c). In contrast to previous calculation,³⁴ no significant shifting of the ligand was observed here. Indeed, 1

and 3 (as well as other guanidylated ligands 4 and 8) were found to adopt a similar orientation inside DOP. This divergence is most likely the result of docking in a flexible receptor (present work) as opposed to a frozen receptor.³⁴ In the latter, it can be hypothesized that the lack of flexibility of the receptor decreased its ability to accommodate the bulkier guanidinium cation. In the IFD model illustrated here, the guanidyl group develops additional stabilizing interactions with the side chains of Asp128, Asn131 and Trp274, supporting the high affinity measured for some compounds bearing this modification (3, 8).

In LENK 1, the β -turn between Gly2 and Leu5 appears to be a bit loose, with a C=O...H–N distance of 2.80 Å. This might be the consequence of the relative positions of the terminal ammonium and carboxylate being pulled away from each other by charged residues within the receptor, with consequential elongation of the β -turn H-bond. Upon replacement of the carboxylate by the larger tetrazole anion, the C-end of compound 2 experiences a slight inward movement to facilitate the fit. This results in a shorter H-bond (2.67 Å). This phenomenon is even further enhanced when the ammonium is replaced by the much bulkier

guanidinium cation in compound 3. In this compound, the β -turn hydrogen bond length is significantly shorter at 2.45 Å.

Replacement of Gly2 by a D-Alanine in compound 5 (Figure 3b and d) does not disrupt the β -turn of LENK. In fact, it rather appeared to stabilize it, as suggested by the very short distance of 2.10 Å for the corresponding H-bond. This stabilization of the active conformation might be a leading cause for the slight increased affinity observed in compounds 5 and 8 ($K_i = 0.36$ and 0.32 nM), when compared to their respective parent compounds 2 and 4 ($K_i = 1.24$ and 1.61 nM), lacking the extra methyl substituents. Note that in this model, the leucine side chain remains within the hydrophobic pocket thought to be responsible for selectivity between MOP and DOP.

Hydrophobicity and Plasma Stability. The next things we were logically concerned about were the physicochemical properties (i.e., lipophilicity and topological polar surface area) and the metabolic stability of the mimetics 2–8, by comparison with the natural ligand LENK 1. First, the lipophilicity of the different mimetics was calculated and evaluated experimentally (Table 1).

Table 1. Measured and Calculated Physicochemical Properties of Analogues 1–8

compd	logD _{7.4} ^a	clogD ^b	tPSA (Å ²) ^b	LLE ^c
1	−1.37	−1.86	204.40	11.20
2	−0.71	−1.57	215.83	9.25
3	−0.42	−1.58	240.40	10.20
4	0.02	−0.13	239.80	9.05
5	0.35	−1.00	215.83	9.25
6	−0.18	−1.57	215.83	8.66
7	−0.07	−1.00	215.83	9.38
8	0.53	0.44	239.80	9.47

^alogD_{7.4} values were measured using the shake-flask method with PBS at pH 7.4. ^bclogD and tPSA were calculated with ChemAxon software. ^cLLE = $-\log\text{EC}_{50}(\text{EPAC}) - \log\text{D}_{7.4}$.

The logD_{7.4} of a compound (C), which is the log of its partition coefficient ($[\text{C}]_{\text{octanol}}/[\text{C}]_{\text{water}}$) at pH 7.4, is acknowledged to be a good index for lipophilicity and BBB permeability.⁶⁶ Measured values (logD_{7.4}) were consistently higher than the calculated clogD,⁶⁷ occasionally by a small margin (8), but more generally by a large gap (1–7). Obviously, the chosen model inadequately considers the structural factors and the weak intramolecular interactions of the molecules.^{68,69} Once again, compound 8 is the most lipophilic, with a gain of almost 2 log units.

Topological polar surface area (tPSA) is the sum of areas of all polar contributions in the molecule, and is therefore an ideal metric for predicting drug transport across the BBB.^{67,70} All compounds were found to have polar surface areas greater than 200 Å², well above the recommended 90 Å² superior limit.^{71,72} However, some peptides with equivalent tPSA are active to the CNS.^{21,73,74} The increase calculated (9–36 Å²) for the synthetic mimetics 2–8, LENK being the reference, can be attributed to the addition of polar atoms in the isostere functions guanidinium and tetrazolate. The logD_{7.4} and tPSA values are useful descriptors for passive permeation, but is worth noting that addition of guanidine groups may favor binding to albumin, thus helping BBB crossing through an active process.^{35,36} Finally, ligand lipophilicity efficiency (LLE) was calculated for each compound, providing a way to evaluate

their potency without their lipophilicity contribution.⁷⁵ Since all LLEs are above 7,⁷⁶ peptides 1–8 are expected to be highly potent ligands.

Plasma stability of compounds 1–8 was then monitored (Figure 2) to provide hints on the metabolic stability of each compound and to study the influence of the four modifications reported here.

On its own, a C-terminal tetrazole did not significantly improve the half-life of compound 2 when compared to LENK 1. This is not surprising, since the main degradation pathway of enkephalins usually involves the first peptide bond.²⁰ Accordingly, this sensitive bond is better protected by a N-terminal guanidyl group in compound 3. When the two terminal modifications are present in a same molecule, as in mimetics 4 and 8, the half-life is significantly increased, as no degradation was observed even after 6 h of incubation in plasma. From the results collected with compounds 2, 5, and 7, one can infer that a Gly² → D-Ala replacement also significantly improved the stability of enkephalins.

CONCLUSION

Novel Leu-enkephalin mimetics have been synthesized, and their pharmacological profiles evaluated. The ammonium and carboxylate ions of Leu-enkephalin have, respectively, been replaced by the similarly charged guanidinium and tetrazolate ions. Side chains (of D conformation) have also been introduced on the α carbon atoms at the second (Gly² → D-Ala) and fifth residues (S *i*-butyl → R *i*-butyl). While no significant DOP/MOP selectivity could be achieved, the guanidinium–tetrazolate combination showed increased plasma stability as well as improved lipophilicity. Among the eight derivatives studied here (including Leu-enkephalin), the best biological properties were obtained for the peptidomimetic 8, bearing the three following modifications: guanidinium and tetrazolate ions plus D-Ala². The affinity and the potency of this compound for DOP and MOP remained similar to that of Leu-enkephalin, but the measured logD_{7.4} was increased by 1.9 log units when compared to Leu-enkephalin, to reach 0.53. Similarly, the sensitivity to degradation was significantly decreased as was already observed with the analogue 4, which also possesses a N-terminal guanidine and a C-terminal tetrazole. Altogether, our results reveal that guanidinium and tetrazole groups can be introduced in opioid peptides to improve their stability and their lipophilicity, without affecting their ability to bind and activate MOP and DOP.

METHODS

Chemistry. For SPPS, commercial grade reagents from Chem Impex were used without further purification. Optical rotation measurements were made on a PerkinElmer 241 polarimeter. ¹H NMR and ¹³C NMR spectra were recorded in deuterated solvents on a Bruker Ascend 400 MHz (100 MHz for ¹³C spectra) or a Bruker Advance 300 Ultrashield 300 MHz (75 MHz for ¹³C spectra) NMR instrument. The residual solvent peaks have been used as internal references. The peak multiplicities are described as follows: s (singlet), d (doublet), t (triplet), q (quartet), quin (quintet), spt (septet), m (multiplet), and br (broad). HRMS were recorded on a Triple TOF 5600 ABSciex mass spectrometer. HPLC preparative purifications were done on a VYDAC 218TP C18 column. HPLC semipreparative purifications were done on a Zorbax Eclipse XDB-C18, 5 μm , 9.4 \times 250 mm column. Analytical HPLCs were done with an Eclipse XDB-C18, 5 μm , 4.6 \times 250 mm column.

(S)-(*9H*-Fluoren-9-yl)methyl (1-Amino-4-methyl-1-oxo-pentan-2-yl)carbamate (**10a**). Fmoc-Leu-OH (**9a**) (2.00 g, 5.6 mmol, 1

equiv), Boc anhydride (1.60 g, 7.35 mmol, 1.3 equiv), and pyridine (0.28 mL, 3.47 mmol, 0.62 equiv) were mixed together in dioxane (7 mL) at room temperature. Ammonium carbonate (0.56 g, 7.13 mmol, 1.26 equiv) was added to the mixture that was stirred at room temperature until completion of the reaction (6 h). EtOAc (30 mL) was added, and the organic layer was washed with water (30 mL) then 5% aqueous H₂SO₄ (30 mL), dried over MgSO₄ and concentrated to dryness. The resulting solid was triturated in Et₂O, and was isolated via filtration to yield the title compound as a pure white solid (1.71 g, 87%). ¹H NMR (300 MHz, DMSO-*d*₆) δ : 7.91 (d, *J* = 7.5 Hz, 2H), 7.74 (d, *J* = 7.0 Hz, 2H), 7.49–7.23 (m, 4H), 6.96 (br s, 1H), 4.39–4.17 (m, 3H), 3.96 (m, 1H), 1.64 (m, 1H), 1.53–1.37 (m, 2H), 0.89 (d, *J* = 6.8 Hz, 3H), 0.87 (d, *J* = 6.8 Hz, 3H). ¹³C NMR (75 MHz, DMSO-*d*₆) δ : 174.9, 156.4, 144.3, 141.2, 128.1, 127.5, 125.8, 120.6, 65.8, 53.4, 47.2, 41.3, 24.8, 23.5, 21.9. Mp 189–190 °C (Et₂O). HRMS (ESI⁺) *m/z* calcd for C₂₁H₂₄N₂O₃ (M + Na)⁺: 375.1679, found: 375.1681, Δ = 0.2 mDa. [α]_D²⁰ –10 (*c* = 5 mg·mL^{–1} in MeOH).

(R)-(9H-Fluoren-9-yl)methyl (1-Amino-4-methyl-1-oxo-pentane-2-yl)carbamate (10b). The same procedure was applied to prepare the enantiomer from Fmoc-D-Leu-OH (**9b**) (yield: 91%). ¹H NMR (300 MHz, DMSO-*d*₆) δ : 7.90 (d, *J* = 7.5 Hz, 2H), 7.73 (d, *J* = 7.0 Hz, 2H), 7.49–7.21 (m, 4H), 6.98 (br s, 1H), 4.41–4.14 (m, 3H), 3.95 (m, 1H), 1.64 (m, 1H), 1.54–1.40 (m, 2H), 0.89 (d, *J* = 6.5 Hz, 3H), 0.87 (d, *J* = 6.5 Hz, 3H). ¹³C NMR (75 MHz, DMSO-*d*₆) δ : 175.0, 156.4, 144.2, 141.2, 128.1, 127.5, 125.8, 120.6, 65.9, 53.4, 47.2, 41.3, 24.7, 23.6, 21.9. HRMS (ESI⁺) *m/z* calcd for C₂₁H₂₄N₂O₃ (M + Na)⁺: 375.1679, found: 375.1688, Δ = 0.9 mDa. [α]_D²⁰ +12 (*c* = 5 mg·mL^{–1} in MeOH).

(S)-(9H-Fluoren-9-yl)methyl (1-Cyano-3-methylbutyl)carbamate (11a). Trifluoroacetic anhydride (0.67 mL, 4.85 mmol, 1.1 equiv) was added dropwise to a solution of the amide **10a** (1.56 g, 4.41 mmol, 1 equiv) and pyridine (0.71 mL, 8.82 mmol, 2 equiv) in dry THF (10 mL) cooled in an ice-bath, in order to keep the internal temperature below 5 °C. The resulting mixture was stirred at room temperature during 16 h, then ice-water was added. The white precipitate that formed was isolated by filtration, rinsed three times with cold water and finally recrystallized in a minimum amount of water to give the title compound as white powder (1.32 g, 89%). ¹H NMR (300 MHz, DMSO-*d*₆) δ : 8.16 (d, *J* = 7.9 Hz, 1H), 7.90 (d, *J* = 7.5 Hz, 2H), 7.70 (d, *J* = 7.5 Hz, 2H), 7.43 (t, *J* = 6.8 Hz, 2H), 7.35 (dt, *J* = 1.1, 7.5 Hz, 2H), 4.57–4.36 (m, 3H), 4.26 (m, 1H), 1.74–1.55 (m, 3H), 0.89 (d, *J* = 6.0 Hz, 3H), 0.88 (d, *J* = 6.0 Hz, 3H). ¹³C NMR (75 MHz, DMSO-*d*₆) δ : 155.9, 144.1, 141.3, 128.1, 127.5, 125.5, 120.6, 120.3, 66.3, 47.1, 41.2, 40.7, 24.7, 22.4, 22.0. Mp 115–117 °C (water). Rf 0.8 (DCM). HRMS (ESI⁺) *m/z* calcd for C₂₁H₂₂N₂O₂ (M + Na)⁺: 357.1573, found: 357.1579, Δ = 0.6 mDa. [α]_D²⁰ –27 (*c* = 5 mg·mL^{–1} in MeOH).

(S)-(9H-Fluoren-9-yl)methyl (1-Cyano-3-methylbutyl)carbamate (11b). The same procedure was applied to prepare the enantiomer from the amide **10b** (yield: 85%). ¹H NMR (300 MHz, DMSO-*d*₆) δ : 8.16 (d, *J* = 7.9 Hz, 1H), 7.90 (d, *J* = 7.5 Hz, 2H), 7.70 (d, *J* = 7.3 Hz, 2H), 7.44 (t, *J* = 6.8 Hz, 2H), 7.33 (dt, *J* = 1.1, 7.5 Hz, 2H), 4.58–4.36 (m, 3H), 4.26 (m, 1H), 1.74–1.54 (m, 3H), 0.89 (d, *J* = 5.9 Hz, 3H), 0.88 (d, *J* = 5.9 Hz, 3H). ¹³C NMR (75 MHz, DMSO-*d*₆) δ : 155.9, 144.1, 141.3, 128.1, 127.5, 125.5, 120.6, 120.3, 66.3, 47.1, 41.2, 40.7, 24.6, 22.4, 22.0. HRMS (ESI⁺) *m/z* calcd for C₂₁H₂₂N₂O₂ (M + Na)⁺: 357.1573, found: 357.1578, Δ = 0.5 mDa. [α]_D²⁰ +31 (*c* = 5 mg·mL^{–1} in MeOH).

(9H-Fluoren-9-yl)methyl (3-Methyl-1-(1H-tetrazol-5-yl) butyl)-carbamate (12a). Cyano (**11a**) (0.97 g, 2.90 mmol, 1 equiv), sodium azide (0.38 g, 5.80 mmol, 2 equiv), and ZnBr₂ (0.33 g, 1.45 mmol, 0.5 equiv) were mixed together in isopropanol/water (10/25 mL) at room temperature. The mixture was heated at 100 °C, and DMF was added until total dissolution. The resulting solution was refluxed for 72 h, and 3 N HCl (10 mL) was added. The precipitate formed was dissolved with the minimum amount of EtOAc. The mixture was extracted with EtOAc (3 × 40 mL). The organic extracts were collected together and washed with brine (50 mL), before being dried over MgSO₄ and concentrated to dryness. The solid was

purified by recrystallization in EtOAc/hexane, to give the title compound as a pure white solid (0.75 g, 89%). ¹H NMR (300 MHz, DMSO-*d*₆) δ : 8.07 (d, *J* = 8.1 Hz, 1H), 7.90 (d, *J* = 7.5 Hz, 2H), 7.72 (t, *J* = 7.0 Hz, 2H), 7.42 (t, *J* = 6.8 Hz, 2H), 7.33 (dt, *J* = 3.0, 7.3 Hz, 2H), 4.95 (m, 1H), 4.35 (m, 2H), 4.24 (m, 1H), 1.91–1.66 (m, 2H), 1.58 (m, 1H), 0.93 (d, *J* = 6.8 Hz, 3H), 0.90 (d, *J* = 6.8 Hz, 3H). ¹³C NMR (75 MHz, DMSO-*d*₆) δ : 156.3, 150.3, 144.2, 141.2, 128.1, 127.5, 125.7, 120.6, 66.1, 47.2, 44.8, 42.2, 24.5, 23.1, 21.9. Mp 191–192 °C (water) HRMS (ESI⁺) *m/z* calcd for C₂₁H₂₃N₅O₂ (M + Na)⁺: 400.1744, found: 400.1751, Δ = 0.7 mDa. [α]_D²⁰ –30 (*c* = 5 mg·mL^{–1} in MeOH).

(9H-Fluoren-9-yl)methyl (3-Methyl-1-(1H-tetrazol-5-yl) butyl)-carbamate (12b). The same procedure was applied to prepare the enantiomer from the cyanide **11b** (yield: 73%). ¹H NMR (300 MHz, DMSO-*d*₆) δ : 8.10 (d, *J* = 8.1 Hz, 1H), 7.88 (d, *J* = 7.3 Hz, 2H), 7.72 (t, *J* = 6.9 Hz, 2H), 7.41 (t, *J* = 6.8 Hz, 2H), 7.30 (m, 2H), 5.00 (m, 1H), 4.51–4.16 (m, 3H), 1.90–1.66 (m, 2H), 1.59 (m, 1H), 0.93 (d, *J* = 6.6 Hz, 3H), 0.90 (d, *J* = 6.6 Hz, 3H). ¹³C NMR (75 MHz, DMSO-*d*₆) δ : 156.3, 150.4, 144.1, 141.2, 127.5, 125.7, 120.6, 66.2, 47.2, 44.9, 42.4, 24.6, 23.1, 21.9. HRMS (ESI⁺) *m/z* calcd for C₂₁H₂₃N₅O₂ (M + Na)⁺: 400.1744, found: 400.1768, Δ = 2.4 mDa. [α]_D²⁰ –27 (*c* = 5 mg·mL^{–1} in MeOH).

General Method for Peptide Synthesis on Solid Support (SPPS Methodology). Between each step, the following sequence of washes was applied: DMF (3×), *i*PrOH (3×) and DCM (3×). For the first coupling, the 2-Cl-trityl resin (624 mg, 0.71 mmol·g^{–1} factory loading) was placed in a sintered glass peptide synthesis vessel and swollen with DCM. The Fmoc protected Leu or **12a** or **12b** (1.2 equiv) and DIPEA (4 equiv) were added to the resin. The suspension was agitated in a shaker for 16 h. The resin was washed with DCM/MeOH/DIPEA (17/2/1). The loading was measured via mass difference after drying the resin. After the initial coupling to the resin, the peptide sequence was then synthesized using conventional SPPS techniques with Fmoc-Phe-OH (coupling #1), Fmoc-Gly-OH (coupling #2), Fmoc-Gly-OH or Fmoc-D-Ala-OH (coupling #3), and Boc-Tyr(*t*Bu)-OH or Fmoc-Tyr(*t*Bu)-OH (coupling #4). All four couplings were performed using 3 equiv of protected amino acid, HATU (3 equiv), and HOBt-Cl (3 equiv), with 9 equiv of DIPEA in a minimum volume of DMF. The resulting suspension was agitated in a shaker for 1 h at a time. This step was repeated until Kaiser's test result was negative. Fmoc deprotections were carried out by suspending then agitating the resin in 20% piperidine in DMF for 5 min (procedure repeated one more time). The final peptides were cleaved off the resin, using 3 mL of cleavage solution per 1 g of resin in a glass vial and with vigorous agitation on a shaker for 3 h. The cleavage solution consisted of 95% TFA, 2.5% H₂O, and 2.5% TIPS. After cleavage, the mixture was filtered on cotton to remove the residual resin. The solvents were concentrated under vacuum and in cold Et₂O (15 mL) was added at 0 °C. The precipitates that formed were centrifuged and the supernatant Et₂O was removed. The remaining precipitates were dissolved in water and *t*BuOH (less than 50%) was added to complete the dissolution if necessary. The final aqueous solutions were frozen and lyophilized. The crude peptides were purified using preparative reverse-phase HPLC (detection at 210 nm), with a C18 column (Solvent A: 0.1% TFA in water and solvent B: 0.1% TFA in acetonitrile. Gradient: 10 to 70% of B in A over 50 min; flow rate: 1 mL/min). The purity of all fractions was analyzed using an analytical HPLC (detection at 210 nm), with a C18 column. All pure fractions (over 96% purity) were combined, frozen, and lyophilized.

General Method for Guanidylation on Solid Support (Concerns Peptides 3, 4, 8). Fmoc-Tyr(*t*Bu)-OH was used instead of Boc-Tyr(*t*Bu)-OH. Fmoc was cleaved as described in the SPPS methodology part. After positive Kaiser test, the resin was swelled in a minimum amount of DCM. A solution of Et₃N (9 equiv) and *N,N*-DiBoc-*N*-methylisothioisourea (1.5 equiv) in DMF (6 mL) was added. The reactor was shaken for 10 min, before adding HgCl₂ (3 equiv) into the solution. The vessel was then agitated for 2 h, or until completion of the reaction monitored by Kaiser test. Sometimes, the reaction needed to be repeated twice to reach completion. The

peptide was then deprotected and cleaved from the resin, as described before.

Peptide 2. ^1H NMR (300 MHz, DMSO- d_6) δ : 8.84–8.66 (m, 2H), 8.19–7.95 (m, 5H), 7.23–7.13 (m, 5H), 7.06 (d, J = 9.5 Hz, 2H), 6.72 (d, J = 9.5 Hz, 2H), 5.22 (m, 1H), 4.54 (m, 1H), 4.01 (m, 1H), 3.90–3.63 (m, 4H), 3.08–2.93 (m, 2H), 2.87–2.65 (m, 2H), 1.87–1.65 (m, 2H), 1.52 (m, 1H), 0.93 (d, J = 6.7 Hz, 3H), 0.85 (d, J = 6.7 Hz, 3H). ^{13}C NMR (75 MHz, D_2O) δ : 172.5, 171.2, 170.7, 169.9, 156.8, 155.2, 135.4, 130.8, 128.9, 128.5, 127.1, 125.4, 115.8, 55.1, 54.5, 42.4, 42.1, 42.0, 40.4, 37.0, 35.9, 24.0, 21.7, 20.7. HRMS (ESI $^+$) m/z calcd for $\text{C}_{28}\text{H}_{37}\text{N}_9\text{O}_5$ ($\text{M} + \text{H}$) $^+$: 602.2812, found: 602.2809, Δ = 0.3 mDa.

Peptide 3. ^1H NMR (400 MHz, D_2O) δ : 7.40–7.23 (m, 5H), 7.15 (d, J = 9.5 Hz, 2H), 6.85 (d, J = 9.5 Hz, 2H), 4.63 (m, 1H), 4.44 (m, 1H), 4.33 (m, 1H), 3.96 and 3.91 (AB, J = 15.8 Hz, 2H), 3.86 (s, 2H), 3.23–3.10 (m, 2H), 3.05–2.93 (m, 2H), 1.68–1.50 (m, 3H), 0.90 (d, J = 6.2 Hz, 3H), 0.84 (d, J = 6.2 Hz, 3H). ^{13}C NMR (100 MHz, D_2O) δ : 176.2, 172.7, 172.2, 171.4, 170.8, 156.5, 154.7, 136.2, 130.7, 129.2, 128.7, 127.3, 127.1, 115.5, 56.5, 54.8, 51.6, 42.5, 42.2, 39.5, 37.2, 36.9, 24.3, 22.1, 20.6. HRMS (ESI $^+$) m/z calcd for $\text{C}_{29}\text{H}_{39}\text{N}_7\text{O}_7$ ($\text{M} + \text{H}$) $^+$: 598.29837, found: 598.3256, Δ = 1.5 mDa.

Peptide 4. ^1H NMR (400 MHz, D_2O) δ : 7.18–7.09 (m, 5H), 7.07–6.98 (m, 2H), 6.83 (d, J = 8.5 Hz, 2H), 5.24 (dd, J = 6.3, 9.6 Hz, 1H), 4.50 (dd, J = 7.1, 8.8 Hz, 1H), 4.44 (dd, J = 5.6, 7.9 Hz, 1H), 3.96 and 3.94 (AB, J = 15.9 Hz, 2H), 3.90 (s, 2H), 3.17 (m, 1H), 3.04–2.84 (m, 3H), 1.81 (m, 1H), 1.64 (m, 1H), 1.45 (m, 1H), 0.86 (d, J = 6.6 Hz, 3H), 0.81 (d, J = 6.6 Hz, 3H). ^{13}C NMR (100 MHz, D_2O) δ : 172.5, 172.2, 171.5, 170.8, 156.8, 156.5, 154.7, 135.4, 130.7, 128.9, 128.5, 127.2, 127.1, 115.5, 56.5, 55.1, 42.6, 42.2, 42.0, 40.3, 37.1, 36.9, 23.9, 21.7, 20.7. HRMS (ESI $^+$) m/z calcd for $\text{C}_{29}\text{H}_{39}\text{N}_{11}\text{O}_5$ ($\text{M} + \text{H}$) $^+$: 622.32084, found: 622.3305, Δ = 9.7 mDa.

Peptide 5. ^1H NMR (300 MHz, D_2O) δ : 7.10–6.98 (m, 5H), 6.97–6.86 (m, 2H), 6.80 (d, J = 8.8 Hz, 2H), 5.14 (m, 1H), 4.41 (m, 1H), 4.16–4.03 (m, 2H), 3.78 (s, 2H), 3.10 (m, 1H), 2.97–2.77 (m, 3H), 1.73 (m, 1H), 1.56 (m, 1H), 1.34 (m, 1H), 1.08 (d, J = 7.3 Hz, 3H), 0.78 (d, J = 6.6 Hz, 3H), 0.73 (d, J = 6.6 Hz, 3H). ^{13}C NMR (75 MHz, D_2O) δ : 174.9, 172.3, 170.7, 169.2, 157.8, 155.1, 135.4, 130.7, 128.9, 128.4, 127.0, 125.5, 115.8, 55.0, 54.5, 49.8, 42.3, 42.1, 40.7, 37.0, 36.0, 24.0, 21.6, 20.8, 16.1. HRMS (ESI $^+$) m/z calcd for $\text{C}_{29}\text{H}_{39}\text{N}_9\text{O}_5$ ($\text{M} + \text{Na}$) $^+$: 616.2966, found: 616.2975, Δ = 0.9 mDa.

Peptide 6. ^1H NMR (300 MHz, D_2O) δ : 7.34–7.20 (m, 3H), 7.19–7.10 (m, 2H), 7.07 (d, J = 8.6 Hz, 2H), 6.81 (d, J = 8.6 Hz, 2H), 5.06 (dd, J = 7.4, 7.9 Hz, 1H), 4.52 (dd, J = 7.5, 7.8 Hz, 1H), 4.18 (t, J = 7.3 Hz, 1H), 3.85 (s, 2H), 3.81 (s, 2H), 3.16–2.84 (m, 4H), 1.53 (m, 2H), 0.96 (m, 1H), 0.73 (d, J = 7.5 Hz, 1H), 0.68 (d, J = 7.5 Hz, 3H). ^{13}C NMR (75 MHz, D_2O) δ : 173.1, 171.2, 170.7, 169.9, 157.7, 155.1, 135.7, 130.8, 129.1, 128.9, 129.1, 128.9, 127.3, 125.5, 115.8, 55.4, 54.5, 43.0, 42.3, 42.1, 40.7, 37.1, 35.9, 23.5, 21.9, 20.5. HRMS (ESI $^+$) m/z calcd for $\text{C}_{28}\text{H}_{37}\text{N}_9\text{O}_5$ ($\text{M} + \text{Na}$) $^+$: 602.2810, found: 602.2819, Δ = 0.9 mDa.

Peptide 7. ^1H NMR (300 MHz, D_2O) δ : 7.33–7.19 (m, 3H), 7.18–7.11 (m, 2H), 7.08 (d, J = 8.5 Hz, 2H), 6.80 (d, J = 8.6 Hz, 2H), 5.06 (m, 1H), 4.49 (m, 1H), 4.15–4.00 (m, 2H), 3.77 (s, 2H), 3.16–2.84 (m, 4H), 1.63–1.41 (m, 2H), 1.07 (d, J = 7.3 Hz, 3H), 0.94 (m, 1H), 0.73 (d, J = 6.6 Hz, 3H), 0.67 (d, J = 6.6 Hz, 3H). ^{13}C NMR (75 MHz, D_2O) δ : 174.9, 173.0, 170.8, 169.2, 157.6, 155.1, 135.7, 130.8, 129.1, 128.8, 127.3, 125.5, 115.8, 55.3, 54.5, 49.8, 43.0, 42.1, 40.6, 37.1, 36.0, 23.5, 21.9, 20.5, 16.1. HRMS (ESI $^+$) m/z calcd for $\text{C}_{29}\text{H}_{39}\text{N}_9\text{O}_5$ ($\text{M} + \text{H}$) $^+$: 616.2966, found: 616.2981, Δ = 1.5 mDa.

Peptide 8. ^1H NMR (400 MHz, D_2O) δ : 7.17–7.07 (m, 5H), 7.05–6.98 (m, 2H), 6.84 (d, J = 8.5 Hz, 2H), 5.23 (dd, J = 6.3, 9.6 Hz, 1H), 4.49 (dd, J = 7.7, 8.5 Hz, 1H), 4.40 (t, J = 6.8 Hz, 1H), 4.21 (q, J = 7.3 Hz, 1H), 3.88 and 3.85 (AB, J = 17.4 Hz, 2H), 3.12–2.85 (m, 4H), 1.81 (m, 1H), 1.64 (m, 1H), 1.45 (m, 1H), 1.28 (d, J = 7.3 Hz, 3H), 0.86 (d, J = 6.6 Hz, 3H), 0.82 (d, J = 6.6 Hz, 3H). ^{13}C NMR (400 MHz, D_2O) δ : 175.2, 172.4, 171.3, 170.8, 156.9, 156.2, 154.7, 135.5, 130.7, 128.9, 128.5, 127.0, 117.7, 115.5, 56.1, 55.0, 50.1, 42.2, 42.0, 40.3, 37.4, 36.8, 23.9, 21.7, 20.6, 16.1. HRMS (ESI $^+$) m/z calcd for $\text{C}_{30}\text{H}_{41}\text{N}_{11}\text{O}_5$ ($\text{M} + \text{H}$) $^+$: 636.33649, found: 636.3409, Δ = 4.4 mDa.

Cell Culture. HEK293 (human embryonic kidney) cells stably expressing the mouse flag-DOP (obtained from Dr Richards Howells, New Jersey Medical School, Newark, NJ) or the human flag-MOP (obtained from Dr. Mark von Zastrow, University of California, San Francisco, CA) were grown at 37 °C in DMEM supplemented with 10% fetal bovine serum and 100 IU/mL penicillin, 100 mg/L streptomycin, and 2 mM glutamine. Geneticin (G418) was added to the medium to maintain the expression of the vector. Cells were grown in humidified atmosphere of 95% air and 5% CO_2 .

Competitive Binding Assays. We evaluated the affinity (K_i) of the different compounds for DOP or MOP using membrane extracts from stable HEK293 cells. HEK293 cells grown to confluence in 150 mm Petri dishes were frozen at –80 °C until use. On the day of the experiment, the cells were submitted to a heat shock by placing the Petri dishes at 37 °C for 60 s before returning to ice. The cells were then harvested in ice-cold buffer A (tris-HCl 20 mM, MgCl_2 5 mM, NaCl 150 mM, pH 7.4) using a cell scraper and centrifuged at 3200g for 15 min at 4 °C. The pellet containing the membrane extract was resuspended in 1 mL of buffer A. The protein concentration was determined with Bio-Rad DC Protein Assay reagents (Bio-Rad Laboratories, Mississauga, ON, Canada), and the pellet was further diluted in buffer A containing 0.01% BSA and distributed in 96-well plates. [^{125}I]-Deltorphin I (specific activity: ~1139 Ci/mmol) or [^{125}I]-DAMGO (specific activity: 2173 Ci/mmol) was used to determine the binding affinity of the compounds in a competitive binding assay on DOP or MOP, respectively. Experiments were performed using a membrane concentration of 50–100 μg of proteins/mL and 150 000 cpm of the radiolabeled ligand. Nonspecific binding was determined using 10 μM nonradioactive deltorphin II or DAMGO. Incubations were performed for 60 min at room temperature with increasing concentration of compound ranging from 10 μM to 1 pM, and the reaction was stopped by filtration using ice-cold buffer A on filtered 96-well plates. Filters were placed in 5 mL tubes, and the radioactivity was determined using a Wizard 2 Automatic Gamma Counter (PerkinElmer, Woodbridge, ON, Canada). Data were analyzed using a nonlinear fitting analysis, and the K_i values were calculated using GraphPad Prism 7.0. K_i are expressed as the mean \pm SEM from three to six independent experiments, each performed in duplicate.

BRET Signaling. HEK293 cells were maintained in DMEM supplemented with 10% FBS, 100 IU/mL penicillin, and 100 μg /mL streptomycin at 37 °C in a humidified atmosphere containing 95% air and 5% CO_2 . The day prior to transfection, cultured cells were washed with PBS at room temperature, trypsinized, and seeded at 3 000 000 cells in a 10 cm Petri dish. For GFP10-EPAC-RLucII transfection, 58 3000 ng of pcDNA3-3HA-ratMOP with 150 ng of GFP10-EPAC-RLucII or 6000 ng of pcDNA3-Flag-ratDOP with 600 ng of GFP10-EPAC-RLucII was added to 600 μL of 150 mM NaCl containing 27 μg of PEI (polyethylenimine) and ssDNA was added to complement to 9 μg the total amount of DNA. For Arr2-GFP10/receptor-RLucII transfection, 600 ng of pcDNA3-3HA-ratMOP-RLucII or pcDNA3-Flag-ratDOP-RLucII with 12000 ng Arr2-GFP10 was added to 600 μL of 150 mM NaCl containing 37.8 μg PEI. The mixture was incubated for 20 min before being added to the cultured cells. At 24 h post-transfection, cells were washed with PBS, trypsinized and plated in 96-well white plates (75 000 cells/well) and left for another 24 h. The cells were then equilibrated at room temperature for at least 1 h with 70 μL stimulation buffer (10 mM Hepes, 1 mM CaCl_2 , 0.5 mM MgCl_2 , 4.2 mM KCl, 146 mM NaCl, 5.5 mM glucose, pH 7.4). Coelenterazine 400A (an RLucII substrate) was added to a final concentration of 5 μM , 10 min before stimulation. For the EPAC assay, cells were first stimulated with 3 μM forskolin to increase cAMP. Cells were stimulated with ligand ranging from 10 μM to 1 pM and incubated for 10 min prior to signal acquisition. BRET2 signals were measured using a TECAN M1000 fluorescence reader (TECAN, Grödig, Austria). RLucII and GFP10 emissions were collected in the 400–450 nm window (RLucII) and 500 to 550 nm window (GFP10). The BRET2 signal was calculated as the ratio of light emitted by the acceptor GFP10 over the light emitted by the donor RLucII. For each assay, data were normalized as

percentage of the maximal Leu-enkephalin response. All data were analyzed using the nonlinear curve fitting equations in GraphPad Prism (v7.0; GraphPad Software, La Jolla, CA) to estimate the pEC_{50} values of the curves for the different pathways. Results are expressed as the mean \pm SEM from 3 to 6 independent experiments, each performed in triplicate.

Molecular Modeling. Calculations were carried out with the Molecular Operating Environment (MOE),⁷⁷ using our model of Leu-enkephalin into the structure of the 1.8 Å human δ -(PDB 4EJ4) opioid 7TM receptor as template. The different modifications were included on LENK with the help of the “builder” tool and the resulting structures were minimized using the OPLS-AA force field. Each resulting ligand (Conformation: “None”) was then docked into the receptor, using the general docking protocol of MOE (Receptor: Receptor + Solvent; Site: Ligand Atoms; Ligand: Ligand Atoms). The “Triangle Matcher” routine (Timeout: 300 s; Returned poses: 1000) was used as placement method, each pose being scored with the “London dG” algorithm (30 retained poses). The different poses were refined with the Induced Fit protocol (Refinement > Induced Fit; Cutoff: 15 Å; Side Chains: Free; Termination Criterion: Gradient 0.01; Iterations: 500; Pharmacophore Restraint: Force Constant 100; Radius offset: 0.4) then scored with the “GBVI/WSA dG” algorithm (5 retained poses). For each peptide, the best pose was then selected based on the best docking score, and visually by the presence of the essential interactions between the phenolic ring and His278 (via two water bridges), and the ammonium (or guanidinium) with Asp128.

LogD_{7.4} Determination. The determination of the distribution coefficient (logD) was performed using a modified version of the shake flask method.²⁷ Before the experiment, octanol and phosphate buffer (PBS pH 7.4) were mixed together for 24 h to allow saturation of each solution. The mixture was allowed to rest, and the 2 phases were separated and used as solvents in the coefficient measurement. Each peptide (0.1 mg) was placed in a vial to which saturated PBS (1 mL) and octanol (0.5 mL) were added. The vial was then shaken mechanically for 10 min. The mixture was allowed to rest for 30 min or until complete phase separation. Aliquots of both phases were taken and injected in an HPLC instrument (10 μ L of each aliquot was injected in an Agilent 1100 series HPLC. Column: Agilent Eclipse Plus C-18 column, 50 mm \times 3.0 mm, 1.8 μ m. Solvent A: 0.1% TFA in water and solvent B: 0.1% TFA in acetonitrile. Gradient: 10 to 90% of B in A over 60 min; flow rate: 0.4 mL/min; UV detection at 210 nm). The retention time of each peptide was already known from the HPLC purity analysis of each peptide. The octanol peak did not interfere with the experiment. The area under the curve (AUC) of the corresponding peak was integrated for each phase injected. The logD for each peptide was calculated as follows: $\log D_{7.4} = \log_{10}(\text{AUC octanol phase}/\text{AUC PBS phase})$.

Plasma Stability. Plasma was prepared from two male Sprague–Dawley rats (300–350 g; Charles River Laboratories, St-Constant, QC, Canada). All animal procedures were approved by the Ethical Committee for Animal Care and Experimentation of the Université de Sherbrooke (protocol #234-14) and were performed in accordance to the regulations of the Canadian Council on Animal Care (CCAC). Briefly, rats were anesthetized with isoflurane (3% isoflurane with 97% medical air) and exsanguinated using an 18G-11/2 needle connected to a vacutainer containing EDTA. The blood was rapidly transferred to 1.5 mL tubes and centrifuged at 1600 g for 15 min at 4 °C. The plasma was then stored at –80 °C in 500 μ L aliquots until use. The stability of Leu-enkephalin and its analogues was determined in plasma diluted to 50% with saline. Therefore, plasma (25 μ L) was incubated at 37 °C for 15 min before the addition of the peptide solution (25 μ L of a 100 μ M isotonic sodium chloride solution; 0.9% w/v). At each indicated time point (0, 1, 2, 5, 10, 15, 20, 30, 60, 120, 180, 240, 300, and 360 min), the aliquot was quenched with 100 μ L of a methanol solution containing 20 μ M Fmoc-Leu-OH as an internal standard. The resulting solutions were centrifuged at 13 000 rpm for 15 min at 4 °C on tubes equipped with 0.2 μ m PVDF centrifugal filters (Canadian Life Science, Peterborough, ON, Canada). A volume of 5 μ L of the resulting supernatant was analyzed on an analytical Water H Class Acquity UPLC coupled with a SQ

detector 2 and a PDA eλ detector (200 to 400 nm) and paired with an Acquity UPLC CSH C18 column, 1.7 μ M, 2.1 Å \sim 50 mm, flow 0.8 mL/min, starting with 0.1% formic acid in water, then to 95% acetonitrile containing 0.1% formic acid in 1.3 min. Area under the curve for the peak corresponding to the extracted mass chromatogram was then measured for both the peptides and the internal standard on the total ion current (TIC) chromatogram and were used for quantification (using the ratio peptide/standard). Values were reported over the 0 min incubation time point to determine the half-life ($t_{1/2}$) using the GraphPad Prism one-phase decay tool. The results are the mean \pm SEM of three independent experiments.

■ ASSOCIATED CONTENT

§ Supporting Information

The Supporting Information is available free of charge on the ACS Publications website at DOI: 10.1021/acscchemneuro.8b00550.

All remaining experimental details, spectral characterization, HPLC analysis, ¹H NMR, and ¹³C NMR spectra for the precursors 10–12 and peptidomimetics 2–8 (PDF)

■ AUTHOR INFORMATION

Corresponding Authors

*E-mail: Brigitte.Guerin2@USherbrooke.ca.

*E-mail: Louis.Gendron@USherbrooke.ca.

*E-mail: Yves.Dory@USherbrooke.ca.

ORCID

Brigitte Guérin: 0000-0002-0319-4512

Louis Gendron: 0000-0002-2058-8863

Yves L. Dory: 0000-0003-4758-1589

Author Contributions

J.-L.B. and V.B. have contributed equally to this work and wrote the original manuscript. B.G., G.P., L.G., and Y.L.D. designed the study and finalized the manuscript through contributions of all authors. All authors have given approval to the final version of the manuscript. J.-L.B., V.B., B.H., and A.B. performed the experiments. J.-L.B. carried out the virtual docking experiments.

Funding

This work was supported by Grants # MOP-102612 and MOP-136871 from the Canadian Institute for Health Sciences (CIHR), awarded to Y.L.D., B.G., G.P., and L.G. L.G. is the recipient of a Senior-salary support from the FRQS. B.G. is holder of the Jeanne and J.-Louis Lévesque Chair in Radiobiology at Université de Sherbrooke. Y.L.D., B.G., and L.G. are members of the FRQS-funded Centre de Recherche du CHUS and of the Institut de Pharmacologie de Sherbrooke. L.G. is a member of CENUS and the FRQS-funded Quebec Pain Research Network (QPRN). L.G. and G.P. are members of the FRQS-funded Réseau québécois de recherche sur le Médicament (RQRM).

Notes

The authors declare no competing financial interest.

■ ACKNOWLEDGMENTS

The authors thank Dr. Richard Howells (Rutgers University-New Jersey Medical School, Newark, NJ) for providing the HEK293 cells expressing the mouse Flag-DOP and Mark von Zastrow (University of California, San Francisco, CA) for the human Flag-MOP.

■ ABBREVIATIONS

DOP, delta opioid receptor; MOP, mu opioid receptor; N-term, N-terminal; C-term, C-terminal; TIS, Trisopropyl Silane; HEK, human embryonic kidney cells; DMF, dimethylformamide; BRET, bioluminescence resonance energy transfer; cAMP, cyclic adenosine monophosphate; GFP, green fluorescent protein; R-luc, Renilla luciferase

■ REFERENCES

- (1) Gaskin, D. J., and Richard, P. (2012) The Economic Costs of Pain in the United States. *J. Pain* 13 (8), 715–724.
- (2) Childers, W. E., Jr, and Baudy, R. B. (2007) N-Methyl-d-Aspartate Antagonists and Neuropathic Pain: The Search for Relief. *J. Med. Chem.* 50 (11), 2557–2562.
- (3) Butera, J. A. (2007) Current and Emerging Targets to Treat Neuropathic Pain. *J. Med. Chem.* 50 (11), 2543–2546.
- (4) Kyle, D. J., and Ilyin, V. I. (2007) Sodium Channel Blockers. *J. Med. Chem.* 50 (11), 2583–2588.
- (5) Munro, G., and Dalby-Brown, W. (2007) Kv7 (KCNQ) Channel Modulators and Neuropathic Pain. *J. Med. Chem.* 50 (11), 2576–2582.
- (6) Schkeryantz, J. M., Kingston, A. E., and Johnson, M. P. (2007) Prospects for Metabotropic Glutamate 1 Receptor Antagonists in the Treatment of Neuropathic Pain. *J. Med. Chem.* 50 (11), 2563–2568.
- (7) Westaway, S. M. (2007) The Potential of Transient Receptor Potential Vanilloid Type 1 Channel Modulators for the Treatment of Pain. *J. Med. Chem.* 50 (11), 2589–2596.
- (8) Bodnar, R. J. (2016) Endogenous Opiates and Behavior: 2014. *Peptides* 75, 18–70.
- (9) Kieffer, B. L. (1999) Opioids: First Lessons from Knockout Mice. *Trends Pharmacol. Sci.* 20 (1), 19–26.
- (10) Beaudry, H., Proteau-Gagné, A., Li, S., Dory, Y., Chavkin, C., and Gendron, L. (2009) Differential Noxious and Motor Tolerance of Chronic Delta Opioid Receptor Agonists in Rodents. *Neuroscience* 161 (2), 381–391.
- (11) Gallant, E. L., and Meert, T. F. (2005) A Comparison of the Antinociceptive and Adverse Effects of the Mu-Opioid Agonist Morphine and the Delta-Opioid Agonist SNC80. *Basic Clin. Pharmacol. Toxicol.* 97 (1), 39–51.
- (12) Mika, J., Przewlocki, R., and Przewlocka, B. (2001) The Role of δ -Opioid Receptor Subtypes in Neuropathic Pain. *Eur. J. Pharmacol.* 415 (1), 31–37.
- (13) Petrillo, P., Angelici, O., Bingham, S., Ficalora, G., Garnier, M., Zaratini, P. F., Petrone, G., Pozzi, O., Sbacchi, M., Stean, T. O., Upton, N., Dondio, G. M., and Scheideler, M. A. (2003) Evidence for a Selective Role of the δ -Opioid Agonist [8R-(4bS*,8a α ,8a β ,12b β)]-7,10-dimethyl-1-methoxy-11-(2-methylpropyl)-oxycarbonyl-5,6,7,8,12,12b-hexahydro-(9H)-4,8-methanobenzofuro-[3,2-e]pyrrolo[2,3-g]isoquinoline Hydrochloride (SB-235863) in Blocking Hyperalgesia Associated with Inflammatory and Neuropathic Pain Responses. *J. Pharmacol. Exp. Ther.* 307 (3), 1079–1089.
- (14) Abdallah, K., and Gendron, L. (2017) The Delta Opioid Receptor in Pain Control. In *Handbook of Experimental Pharmacology*, pp 1–31, Springer, Berlin, Heidelberg.
- (15) Gavériaux-Ruff, C., and Kieffer, B. L. (2011) Delta Opioid Receptor Analgesia: Recent Contributions from Pharmacology and Molecular Approaches. *Behav. Pharmacol.* 22 (5 and 6), 405–414.
- (16) Vanderah, T. W. (2010) Delta and Kappa Opioid Receptors as Suitable Drug Targets for Pain. *Clin. J. Pain* 26, S10.
- (17) Le Bourdonnec, B., Windh, R. T., Ajello, C. W., Leister, L. K., Gu, M., Chu, G.-H., Tuthill, P. A., Barker, W. M., Koblish, M., Wiant, D. D., Graczyk, T. M., Belanger, S., Cassel, J. A., Feschenko, M. S., Brogdon, B. L., Smith, S. A., Christ, D. D., Derelanko, M. J., Kutz, S., Little, P. J., DeHaven, R. N., DeHaven-Hudkins, D. L., and Dolle, R. E. (2008) Potent, Orally Bioavailable Delta Opioid Receptor Agonists for the Treatment of Pain: Discovery of NN-Diethyl-4-(5-hydroxy-2,4'-piperidine)-4-yl) benzamide (ADLS859). *J. Med. Chem.* 51 (19), 5893–5896.
- (18) Le Bourdonnec, B., Windh, R. T., Leister, L. K., Zhou, Q. J., Ajello, C. W., Gu, M., Chu, G.-H., Tuthill, P. A., Barker, W. M., Koblish, M., Wiant, D. D., Graczyk, T. M., Belanger, S., Cassel, J. A., Feschenko, M. S., Brogdon, B. L., Smith, S. A., Derelanko, M. J., Kutz, S., Little, P. J., DeHaven, R. N., DeHaven-Hudkins, D. L., and Dolle, R. E. (2009) Spirocyclic Delta Opioid Receptor Agonists for the Treatment of Pain: Discovery of NN-Diethyl-3-hydroxy-4-(spiro-[chromene-2,4'-piperidine]-4-yl) Benzamide (ADLS747). *J. Med. Chem.* 52 (18), 5685–5702.
- (19) Spahn, V., and Stein, C. (2017) Targeting Delta Opioid Receptors for Pain Treatment: Drugs in Phase I and II Clinical Development. *Expert Opin. Invest. Drugs* 26 (2), 155–160.
- (20) Roques, B. P., Noble, F., Dauge, V., Fournié-Zaluski, M. C., and Beaumont, A. (1993) Neutral Endopeptidase 24.11: Structure, Inhibition, and Experimental and Clinical Pharmacology. *Pharmacol. Rev.* 45 (1), 87–146.
- (21) Nielsen, D. S., Shepherd, N. E., Xu, W., Lucke, A. J., Stoermer, M. J., and Fairlie, D. P. (2017) Orally Absorbed Cyclic Peptides. *Chem. Rev.* 117 (12), 8094–8128.
- (22) Mosberg, H. I., Hurst, R., Hruby, V. J., Gee, K., Yamamura, H. I., Galligan, J. J., and Burks, T. F. (1983) Bis-Penicillamine Enkephalins Possess Highly Improved Specificity toward Delta Opioid Receptors. *Proc. Natl. Acad. Sci. U. S. A.* 80 (19), 5871–5874.
- (23) Mosberg, H. I., Omnaas, J. R., Medzihradsky, F., and Smith, C. B. (1988) Cyclic, Disulfide- and Dithioether-Containing Opioid Tetrapeptides: Development of a Ligand with High Delta Opioid Receptor Selectivity and Affinity. *Life Sci.* 43 (12), 1013–1020.
- (24) Proteau-Gagné, A., Bournival, V., Rochon, K., Dory, Y. L., and Gendron, L. (2010) Exploring the Backbone of Enkephalins to Adjust their Pharmacological Profile for the δ -Opioid Receptor. *ACS Chem. Neurosci.* 1 (11), 757–769.
- (25) Proteau-Gagné, A., Rochon, K., Roy, M., Albert, P.-J., Guérin, B., Gendron, L., and Dory, Y. L. (2013) Systematic Replacement of Amides by 1,4-Disubstituted[1,2,3]Triazoles in Leu-Enkephalin and the Impact on the Delta Opioid Receptor Activity. *Bioorg. Med. Chem. Lett.* 23 (19), 5267–5269.
- (26) Rochon, K., Proteau-Gagné, A., Bourassa, P., Nadon, J.-F., Côté, J., Bournival, V., Gobeil, F., Guérin, B., Dory, Y. L., and Gendron, L. (2013) Preparation and Evaluation at the Delta Opioid Receptor of a Series of Linear Leu-Enkephalin Analogues Obtained by Systematic Replacement of the Amides. *ACS Chem. Neurosci.* 4 (8), 1204–1216.
- (27) Nadon, J.-F., Rochon, K., Grastilleur, S., Langlois, G., Dao, T. H., Blais, V., Guérin, B., Gendron, L., and Dory, Y. L. (2017) Synthesis of Gly- ψ [(Z)CF=CH]-Phe, a Fluoroalkene Dipeptide Isostere, and Its Incorporation into a Leu-Enkephalin Peptidomimetic. *ACS Chem. Neurosci.* 8 (1), 40–49.
- (28) Karad, S. N., Pal, M., Crowley, R. S., Prisinzano, T. E., and Altman, R. A. (2017) Synthesis and Opioid Activity of Tyr¹- ψ [(Z)CF=CH]-Gly² and Tyr¹- ψ [(S)/(R)-CF₃CH-NH]-Gly² Leu-Enkephalin Fluorinated Peptidomimetics. *ChemMedChem* 12 (8), 571–576.
- (29) Manturewicz, M., Kosson, P., and Grzonka, Z. (2007) Syntheses of Fmoc- α -aminoalkyltetrazoles and Tetrazole Analogue of Leu-Enkephalin. *Polym. J. Chem.* 81 (7), 1327–1334.
- (30) Poras, H., Bonnard, E., Dangé, E., Fournié-Zaluski, M.-C., and Roques, B. P. (2014) New Orally Active Dual Enkephalinase Inhibitors (DENKIs) for Central and Peripheral Pain Treatment. *J. Med. Chem.* 57 (13), 5748–5763.
- (31) Granier, S., Manglik, A., Kruse, A. C., Kobilka, T. S., Thian, F. S., Weis, W. I., and Kobilka, B. K. (2012) Structure of the δ -Opioid Receptor Bound to Naltrindole. *Nature* 485 (7398), 400–404.
- (32) Wu, H., Wacker, D., Mileni, M., Katritch, V., Han, G. W., Vardy, E., Liu, W., Thompson, A. A., Huang, X.-P., Carroll, F. I., Mascarella, S. W., Westkaemper, R. B., Mosier, P. D., Roth, B. L., Cherezov, V., and Stevens, R. C. (2012) Structure of the Human κ -Opioid Receptor in Complex with JDTic. *Nature* 485 (7398), 327–332.
- (33) Huang, W., Manglik, A., Venkatakrishnan, A. J., Laeremans, T., Feinberg, E. N., Sanborn, A. L., Kato, H. E., Livingston, K. E.,

- Thorsen, T. S., Kling, R. C., Granier, S., Gmeiner, P., Husbands, S. M., Traynor, J. R., Weis, W. I., Steyaert, J., Dror, R. O., and Kobilka, B. K. (2015) Structural Insights into μ -Opioid Receptor Activation. *Nature* 524 (7565), 315–321.
- (34) Weltrowska, G., Nguyen, T. M.-D., Chung, N. N., Wilkes, B. C., and Schiller, P. W. (2013) N-Terminal Guanidinylation of TIPP (Tyr-Tic-Phe-Phe) Peptides Results in Major Changes of the Opioid Activity Profile. *Bioorg. Med. Chem. Lett.* 23 (18), 5082–5085.
- (35) Kumagai, A. K., Eisenberg, J. B., and Pardridge, W. M. (1987) Absorptive-Mediated Endocytosis of Cationized Albumin and a Beta-Endorphin-Cationized Albumin Chimeric Peptide by Isolated Brain Capillaries. Model System of Blood-Brain Barrier Transport. *J. Biol. Chem.* 262 (31), 15214–15219.
- (36) Hau, V. S., Huber, J. D., Campos, C. R., Lipkowski, A. W., Misicka, A., and Davis, T. P. (2002) Effect of Guanidino Modification and Proline Substitution on the in Vitro Stability and Blood–Brain Barrier Permeability of Endomorphin II. *J. Pharm. Sci.* 91 (10), 2140–2149.
- (37) Bańkowski, K., Michalak, O. M., Leśniak, A., Filip, K. E., Cmoch, P., Szewczuk, Z., Stefanowicz, P., and Izdebski, J. (2015) N-Terminal Guanidinylation of the Cyclic 1,4-Ureido-Deltorphin Analogues: The Synthesis, Receptor Binding Studies, and Resistance to Proteolytic Digestion. *J. Pept. Sci.* 21 (6), 467–475.
- (38) Liu, H.-M., Liu, X.-F., Yao, J.-L., Wang, C.-L., Yu, Y., and Wang, R. (2006) Utilization of Combined Chemical Modifications to Enhance the Blood-Brain Barrier Permeability and Pharmacological Activity of Endomorphin-1. *J. Pharmacol. Exp. Ther.* 319 (1), 308–316.
- (39) Beddell, C. R., Clark, R. B., Hardy, G. W., Lowe, L. A., Ubatuba, F. B., Vane, J. R., and Wilkinson, S. (1977) Structural Requirements for Opioid Activity of Analogues of the Enkephalins. *Proc. R. Soc. London B Biol. Sci.* 198 (1132), 249–265.
- (40) Gacel, G., Fournie-Zaluski, M.-C., and Roques, B. P. (1980) D-Tyr–Ser–Gly–Phe–Leu–Thr, a Highly Preferential Ligand for δ -Opiate Receptors. *FEBS Lett.* 118 (2), 245–247.
- (41) Zajac, J.-M., Gacel, G., Petit, F., Dodey, P., Rossignol, P., and Roques, B. P. (1983) Deltakephalin, Tyr-D-Thr-Gly-Phe-Leu-Thr: A New Highly Potent and Fully Specific Agonist for Opiate δ -Receptors. *Biochem. Biophys. Res. Commun.* 111 (2), 390–397.
- (42) Hughes, J., Smith, T. W., Kosterlitz, H. W., Fothergill, L. A., Morgan, B. A., and Morris, H. R. (1975) Identification of Two Related Pentapeptides from the Brain with Potent Opiate Agonist Activity. *Nature* 258 (5536), 577–580.
- (43) Thanawala, V., Kadam, V. J., and Ghosh, R. (2008) Enkephalinase Inhibitors: Potential Agents for the Management of Pain. *Curr. Drug Targets* 9 (10), 887–894.
- (44) Lyons, P. J., Callaway, M. B., and Fricker, L. D. (2008) Characterization of Carboxypeptidase A6, an Extracellular Matrix Peptidase. *J. Biol. Chem.* 283 (11), 7054–7063.
- (45) Benuck, M., Berg, M. J., and Marks, N. (1982) Separate Metabolic Pathways for Leu-Enkephalin and Met-Enkephalin-Arg⁶-Phe⁷ Degradation by Rat Striatal Synaptosomal Membranes. *Neurochem. Int.* 4 (5), 389–396.
- (46) Hersh, L. B. (1982) Degradation of Enkephalins: The Search for an Enkephalinase. *Mol. Cell. Biochem.* 47 (1), 35–43.
- (47) Sureshbabu, V. V., Venkataramanarao, R., Naik, S. A., and Chennakrishnareddy, G. (2007) Synthesis of Tetrazole Analogues of Amino Acids Using Fmoc Chemistry: Isolation of Amino Free Tetrazoles and Their Incorporation into Peptides. *Tetrahedron Lett.* 48 (39), 7038–7041.
- (48) Gunn, S. J., Baker, A., Bertram, R. D., and Warriner, S. L. (2007) A Novel Approach to the Solid-Phase Synthesis of Peptides with a Tetrazole at the C-Terminus. *Synlett* 2007 (17), 2643–2646.
- (49) Bionda, N., Pitteloud, J.-P., and Cudic, P. (2013) Solid-Phase Synthesis of Fusaricidin/Li-F Class of Cyclic Lipopeptides: Guanidinylation of Resin-Bound Peptidyl Amines. *Biopolymers* 100 (2), 160–166.
- (50) Stawikowski, M., and Cudic, P. (2006) A Novel Strategy for the Solid-Phase Synthesis of Cyclic Lipopeptides. *Tetrahedron Lett.* 47 (48), 8587–8590.
- (51) Diss, M. L., and Kennan, A. J. (2008) Orthogonal Recognition in Dimeric Coiled Coils via Buried Polar-Group Modulation. *J. Am. Chem. Soc.* 130 (4), 1321–1327.
- (52) Yong, Y. F., Kowalski, J. A., and Lipton, M. A. (1997) Facile and Efficient Guanidinylation of Amines Using Thioureas and Mukaiyama's Reagent. *J. Org. Chem.* 62 (5), 1540–1542.
- (53) Ohara, K., Vasseur, J.-J., and Smietana, M. (2009) NIS-Promoted Guanidinylation of Amines. *Tetrahedron Lett.* 50 (13), 1463–1465.
- (54) Yong, Y. F., Kowalski, J. A., Thoen, J. C., and Lipton, M. A. (1999) A New Reagent for Solid and Solution Phase Synthesis of Protected Guanidines from Amines. *Tetrahedron Lett.* 40 (1), 53–56.
- (55) Schneider, S. E., Bishop, P. A., Salazar, M. A., Bishop, O. A., and Anslyn, E. V. (1998) Solid Phase Synthesis of Oligomeric Guanidiniums. *Tetrahedron* 54 (50), 15063–15086.
- (56) Gendron, L., Cahill, C. M., von Zastrow, M., Schiller, P. W., and Pineyro, G. (2016) Molecular Pharmacology of δ -Opioid Receptors. *Pharmacol. Rev.* 68 (3), 631–700.
- (57) Quock, R. M., Burkey, T. H., Varga, E., Hosohata, Y., Hosohata, K., Cowell, S. M., Slate, C. A., Ehler, F. J., Roeske, W. R., and Yamamura, H. I. (1999) The Delta-Opioid Receptor: Molecular Pharmacology, Signal Transduction, and the Determination of Drug Efficacy. *Pharmacol. Rev.* 51 (3), 503–532.
- (58) Breton, B., Sauvageau, E., Zhou, J., Bonin, H., Le Gouill, C., and Bouvier, M. (2010) Multiplexing of Multicolor Bioluminescence Resonance Energy Transfer. *Biophys. J.* 99 (12), 4037–4046.
- (59) Audet, N., Charfi, I., Mnie-Filali, O., Amraei, M., Chabot-Doré, A.-J., Millecamps, M., Stone, L. S., and Pineyro, G. (2012) Differential Association of Receptor-G $\beta\gamma$ Complexes with β -Arrestin2 Determines Recycling Bias and Potential for Tolerance of Delta Opioid Receptor Agonists. *J. Neurosci.* 32 (14), 4827–4840.
- (60) Xiang, B., Yu, G.-H., Guo, J., Chen, L., Hu, W., Pei, G., and Ma, L. (2001) Heterologous Activation of Protein Kinase C Stimulates Phosphorylation of δ -Opioid Receptor at Serine 344, Resulting in β -Arrestin- and Clathrin-Mediated Receptor Internalization. *J. Biol. Chem.* 276 (7), 4709–4716.
- (61) Bohn, L. M., Lefkowitz, R. J., Gainetdinov, R. R., Peppel, K., Caron, M. G., and Lin, F.-T. (1999) Enhanced Morphine Analgesia in Mice Lacking β -Arrestin 2. *Science* 286 (5449), 2495–2498.
- (62) Bohn, L. M., Gainetdinov, R. R., Lin, F. T., Lefkowitz, R. J., and Caron, M. G. (2000) Mu-Opioid Receptor Desensitization by Beta-Arrestin-2 Determines Morphine Tolerance but Not Dependence. *Nature* 408 (6813), 720–723.
- (63) Raehal, K. M., Walker, J. K. L., and Bohn, L. M. (2005) Morphine Side Effects in β -Arrestin 2 Knockout Mice. *J. Pharmacol. Exp. Ther.* 314 (3), 1195–1201.
- (64) Altarifi, A. A., David, B., Muchhala, K. H., Blough, B. E., Akbarali, H., and Negus, S. S. (2017) Effect of Acute and Repeated Treatment with the Biased Mu Opioid Receptor Agonist TRV130 (Oliceridine) on Measures of Antinociception, Gastrointestinal Function, and Abuse Liability in Rodents. *J. Psychopharmacol.* 31 (6), 730–739.
- (65) Hill, R., Disney, A., Conibear, A., Sutcliffe, K., Dewey, W., Husbands, S., Bailey, C., Kelly, E., and Henderson, G. (2018) The Novel μ -Opioid Receptor Agonist PZM21 Depresses Respiration and Induces Tolerance to Antinociception. *Br. J. Pharmacol.* 175 (13), 2653–2661.
- (66) Clark, D. E. (2003) In Silico Prediction of Blood–Brain Barrier Permeation. *Drug Discovery Today* 8 (12), 927–933.
- (67) MarvinSketch, version 16.9.26.0, Calculation Module Developed by ChemAxon, <http://www.chemaxon.com/products/marvin/marvinsketch>, 2018 March 7.
- (68) Kowol, C. R., Miklos, W., Pfaff, S., Hager, S., Kallus, S., Pelivan, K., Kubanik, M., Enyedy, E. A., Berger, W., Heffeter, P., and Keppler, B. K. (2016) Impact of Stepwise NH₂-Methylation of Triapine on the

Physicochemical Properties, Anticancer Activity, and Resistance Circumvention. *J. Med. Chem.* 59 (14), 6739–6752.

(69) Donovan, S. F., and Pescatore, M. C. (2002) Method for Measuring the Logarithm of the Octanol–Water Partition Coefficient by Using Short Octadecyl–Poly(Vinyl Alcohol) High-Performance Liquid Chromatography Columns. *J. Chromatogr. A* 952 (1), 47–61.

(70) Ertl, P., Rohde, B., and Selzer, P. (2000) Fast Calculation of Molecular Polar Surface Area as a Sum of Fragment-Based Contributions and Its Application to the Prediction of Drug Transport Properties. *J. Med. Chem.* 43 (20), 3714–3717.

(71) Pajouhesh, H., and Lenz, G. R. (2005) Medicinal Chemical Properties of Successful Central Nervous System Drugs. *NeuroRx* 2 (4), 541–553.

(72) Veber, D. F., Johnson, S. R., Cheng, H.-Y., Smith, B. R., Ward, K. W., and Kopple, K. D. (2002) Molecular Properties that Influence the Oral Bioavailability of Drug Candidates. *J. Med. Chem.* 45 (12), 2615–2623.

(73) Ballet, S., Misicka, A., Kosson, P., Lemieux, C., Chung, N. N., Schiller, P. W., Lipkowski, A. W., and Tourwé, D. (2008) Blood–Brain Barrier Penetration by Two Dermorphin Tetrapeptide Analogues: Role of Lipophilicity vs Structural Flexibility. *J. Med. Chem.* 51 (8), 2571–2574.

(74) Starnowska, J., Costante, R., Guillemyn, K., Popielek-Barczyk, K., Chung, N. N., Lemieux, C., Keresztes, A., Van Duppen, J., Mollica, A., Streicher, J., et al. (2017) Analgesic Properties of Opioid/NK1 Multitarget Ligands with Distinct in Vitro Profiles in Naive and Chronic Constriction Injury Mice. *ACS Chem. Neurosci.* 8 (10), 2315–2324.

(75) Hopkins, A. L., Keserü, G. M., Leeson, P. D., Rees, D. C., and Reynolds, C. H. (2014) The Role of Ligand Efficiency Metrics in Drug Discovery. *Nat. Rev. Drug Discovery* 13 (2), 105–121.

(76) De Marco, R., Bedini, A., Spampinato, S., and Gentilucci, L. (2014) Synthesis of Tripeptides Containing D-Trp Substituted at the Indole Ring, Assessment of Opioid Receptor Binding and in Vivo Central Antinociception. *J. Med. Chem.* 57 (15), 6861–6866.

(77) *Molecular Operating Environment (MOE)*, 2013.08, Chemical Computing Group ULC: Montreal, QC, Canada, 2018.